

FAILURE OF EQUINE COMPACT BONE UNDER IMPACT LOADING

M. Shazly¹, R. Kayacan², V. Prakash¹, C. Rimnac¹, D. Davy¹

¹Department of Mechanical and Aerospace Engineering, Case Western Reserve University, Cleveland, OH, 44106, USA

²Department of Mechanical Engineering, Suleyman Demirel University, Isparta, Turkey

ABSTRACT

In this study we investigated the failure of compact bone under high speed compressive loading using a split Hopkinson pressure bar (SHPB). Cylindrical samples 6.3 mm in diameter and 4 mm long were obtained from equine metacarpals. The stress-strain behavior was compared to that at quasi-static loading. For the SHPB samples, the average yield and ultimate stresses were more than two times greater and the average yield strain was about half compared to the quasi-statically loaded samples. The SHPB samples rapidly dropped to zero loading after reaching a maximum stress, and high speed video images demonstrated that the SHPB samples disintegrated explosively following the drop off of load. In contrast, the quasi-statically loaded samples typically maintained a load plateau following initial load drop off. The results suggest that the time-dependent damage accumulation processes that are known to be active at slower loading rates are not active to any degree in the impact loading situation.

1 INTRODUCTION

The strength of bone is known to be dependent on the rate of loading. Over a range of loading rates consistent with normal physiological loads, the effects of loading rate on mechanical properties such as stiffness, yield strength, ultimate stress and toughness, vary modestly with rate [1-3]. However, in impact loading situations, strength and stiffness can increase considerably [4, 5]. Bone is a complex composite material that demonstrates behaviors associated with viscoelasticity, viscoplasticity and damage accumulation. Under impact loading conditions, the evolution of these inelastic processes and their role in controlling the deformation process is presently not well understood. In view of this, the present study is undertaken to examine the dynamic deformation and failure processes in equine compact bone by examining the compressive stress-strain behavior of cortical bone under high speed loading using a split Hopkinson pressure bar (SHPB) and comparing that behavior to similar samples loaded in quasi-static compression. We examined the effects on mechanical properties including yield stress, yield strain, ultimate stress and stiffness. We also captured the failure process in the SHPB using high speed photography to look for evidence of the failure mechanisms during high speed compressive loading.

2 METHODS

For a source of cortical bone, we obtained fresh fore-limb canon bones (third metacarpal) of horses at autopsy (Ohio State School of Veterinary Medicine). Four millimeter thick strips of bone oriented transversely to the long axis of the bone were machined from the mid-regions (diaphyses) of the bones. The strips were first cut using a table-top CNC milling machine, and then ground by hand to the final 4 mm thickness. From these strips were machined using a diamond coring axis to produce specimens 6.3 mm in dia. and 4.0 mm in length, with axes oriented along the long axis of the bone. All specimens were maintained wet by a water drip during machining and were stored at -20°C until testing.

A Split Hopkinson Pressure Bar (SHPB) was employed to conduct the high strain rate compression tests. The schematic of the SHPB facility at CWRU is shown in Figure 1. The apparatus comprises a striker, an incident and a transmitter bar made from high strength 7075-T6

Al alloy (nominal yield strength 500 MPa) and having a diameter of 19.05 mm. In the present experiments striker bars of lengths varying from 0.05 m to 0.3 m were employed, while the incident and transmitted bars were 1.8 m long. The striker bar is accelerated using an air operated gas gun. A pair of foil strain gages (Measurements Group WK-06-250BF-10C) are strategically attached on the incident bar while a pair of semiconductor strain gages (BLH SPB3-18-100-U1) are attached on the transmitted bar. These strain gages are used in conjunction with Wheatstone bridge circuits, the output of which are amplified by a differential amplifier (Tektronix 5A22N) and recorded on a digital oscilloscope (Tektronix TDS 420) to monitor the strain during the test. The impact velocity of the striker bar was varied from 7 to 15 m/sec so as to obtain strain rates in the range 300s^{-1} to 1300s^{-1} . To understand the dynamic failure process of the equine bone, a high speed camera, Hadland ULTRA 17, with a framing rate of 150,000/sec was. Along with the high strain rate tests quasi-static tests (10^{-5} - 10^{-2}) were also conducted to facilitate comparison with the high strain rate data. The quasi-static tests were tested using a Shenck Pegasus hydraulic test rig equipped with a 100 kN load cell.

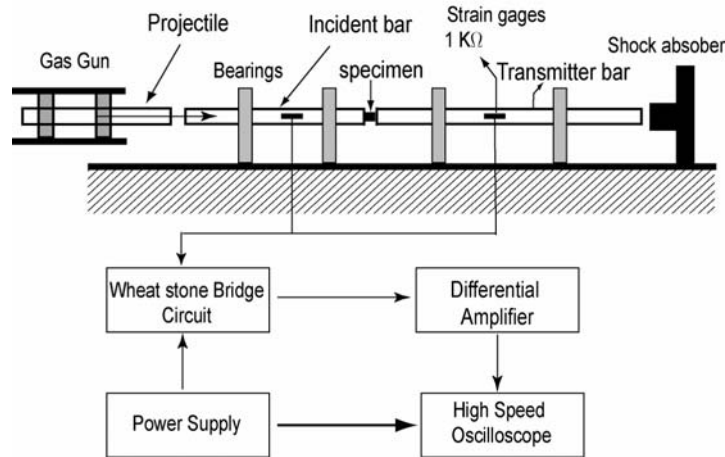


Figure 1: Schematic of Split-Hopkinson Bar used to conduct the dynamic compression tests.

3 RESULTS

The results of the dynamic and quasi-static tests are summarized in Figure 2. The strength and stiffness of the equine bone samples under high speed loading were dramatically greater than those obtained under slow speed loading. The average ultimate stress for the dynamically loaded samples was $391.5 (\pm 26.5)$ standard deviation) MPa and for the quasi-statically loaded samples were $174.2 (\pm 10.1)$ MPa and $214 (\pm 8)$ MPa at strain rates of $8 \times 10^{-5}/\text{sec}$ and $1.7 \times 10^{-2}/\text{sec}$, respectively. The average yield stress based on a 0.2% offset for the SHPB loaded samples was $310.9 (\pm 25.9)$ MPa and for the quasi-statically loaded samples were $153.3 (\pm 14.6)$ MPa and $179 (\pm 13.8)$ MPa at strain rates of $8 \times 10^{-5}/\text{sec}$ and $1.7 \times 10^{-2}/\text{sec}$, respectively. The corresponding average yield strain for the dynamically loaded samples was $0.731\% (\pm 14\%)$ and for the quasi-statically loaded samples were $1.81\% (\pm 05\%)$ and $1.61\% (\pm 425\%)$ at strain rates of $8 \times 10^{-5}/\text{sec}$ and $1.7 \times 10^{-2}/\text{sec}$, respectively. The stiffness, based on the slope of the stress versus strain curves over the load range 10% to 40% of the maximum load, was $61.33 (\pm 13.19)$ GPa under dynamic loading conditions and were $9.36 (\pm 1.73)$ GPa and $15.23 (\pm 3.7)$ GPa at strain rates of $8 \times 10^{-5}/\text{sec}$ and $1.7 \times 10^{-2}/\text{sec}$, respectively.

Moreover, under dynamic loading conditions, the stress after reaching a maximum, drops rapidly to essentially zero. This is in contrast to the quasi-statically loaded samples, which typically displayed a relatively long, extended plateau following the initial drop after reaching the peak stress.

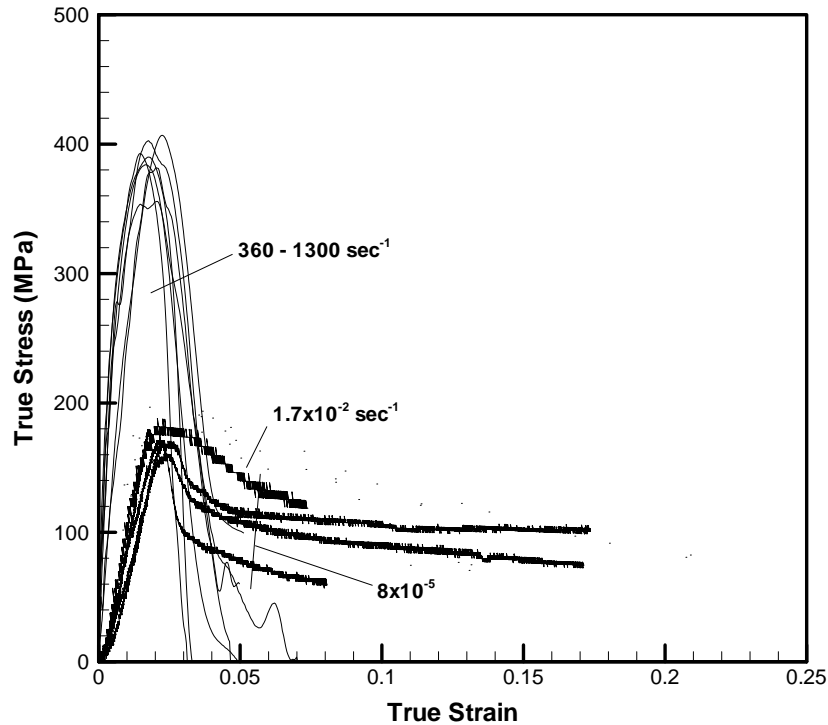


Figure 2: Dynamic vs. quasi-static compression loading of equine bone

Figures 3 and 4 represent selected high speed camera frames showing the dynamic failure processes in equine bone. In all experiments the samples are consistently observed to attain a peak stress at a time of $27.6 (\pm 2.06)$ microseconds after the arrival of the stress pulse at the specimen. The high speed photography indicates a rapid disintegration of the bone samples under the uniaxial stress loading. Comparison of the stress histories and the video records indicate that all ability to sustain load preceded sample disintegration by several tens of microseconds. In fact, the first evidence of gross deformation prior to failure occurred on an average at $64.1 (\pm 25.9)$ microseconds after the arrival of the stress pulse at the specimen. It is interesting to note that the specimen in Figure 3 failed by mushrooming at one end. The failure in the specimen shown in Figure 4, which was more typical, appears to initiate at one end, but shows a general disintegration along its length. All other failures had features of these two, and a few samples showed some evidence of buckling during gross failure.

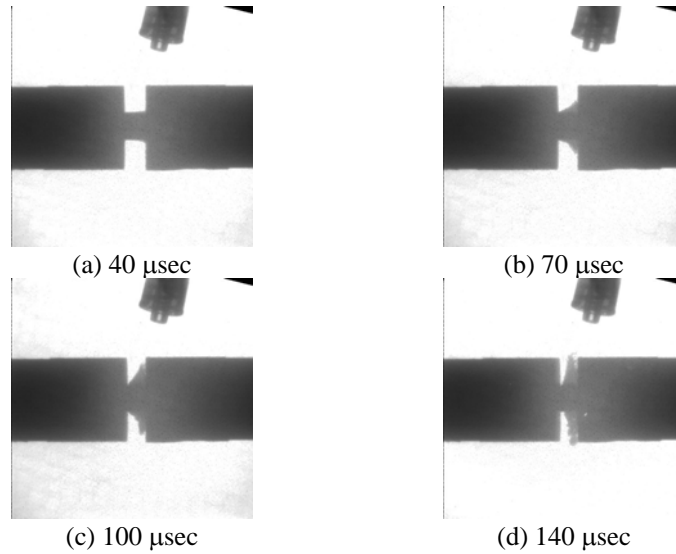


Figure 3: Selected high speed camera frames showing one of the failure processes of equine bone. Times after the arrival of the stress pulse at the specimen

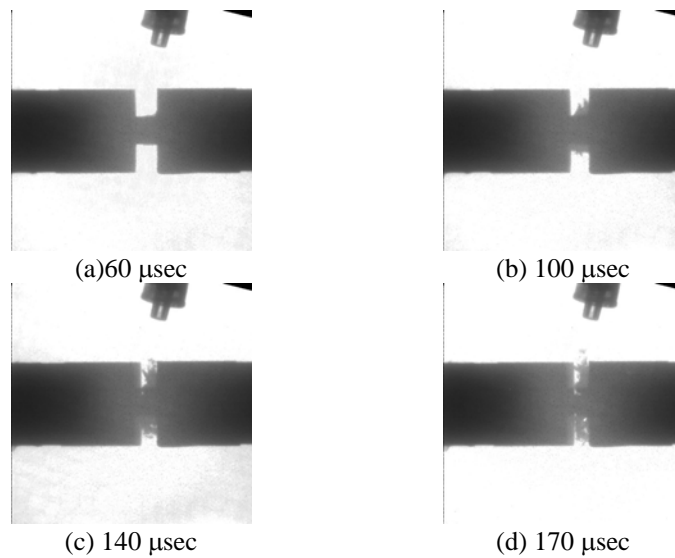


Figure 4: Selected high speed camera frames showing second type of the failure processes of equine bone. Times after the arrival of the stress pulse at the specimen

4. DISCUSSION

The high speed loading of cortical bone demonstrated much greater values for typical measures of stiffness and strength compared to slow (quasi-static) loading. The results for equine bone are in line with the limited amount of data that have been published on this phenomenon. Early data for embalmed human cortical bone indicated stiffness and ultimate compressive stress at impact loading rates (1500/sec) were more than double the values at very slow rates (0.001/sec) [4]. In other work Lewis and Goldsmith found similar increases in strength with rate for human bone, but found much smaller increases in modulus with rate [5]

The present work also shows phenomena that, to our knowledge, have not been previously reported. In particular, the results from the SHPB tests showed there is a complete loss of load carrying ability under high speed loading. Typically, the load fell to zero at a rate similar to the rate at which the load increased (Figure 2). In contrast the quasi-statically loaded samples typically showed an initial drop followed by a plateau at a significant load (Figure 2). This latter result is consistent with reported results showing machined cortical bone samples sustaining substantial compressive loads well beyond the deformations associated with the maximum stress [6-8].

We also found that the drop to zero loading in the SHPB tests occurred a significant time before any evidence of the failure was apparent on the high speed camera records. This suggests that the material integrity is fully lost before any significant movement of the material occurs. After deformation of the sample becomes evident visually, a great deal of fragmentation of the sample accompanies the crushing down of the sample. The video records suggest that the primary failure of the bone is via the splitting and buckling of the structure. We did not examine the micro structure of compact equine bone, which would be expected to contain both osteonal regions and some primary lamellar bone. Both types would offer numerous inter-lamellar interfaces. In addition, there are the cement lines that demarcate the osteons and interstitial material, which is comprised of fragments of old osteons or old primary bone. All of these tissue types offer a number of longitudinal interfaces along which splitting or buckling could occur.

It is not possible to determine from the destructive tests the role damage accumulation plays in the failure process at high speeds. We have previously hypothesized that damage plays a primary role in the nonlinear stress-strain behavior of bone when loaded at physiological rates [9, 10]. This damage may occur at several possible scales. In addition to the micro-structure described above, bone has additional structure at the nano-scale, specifically collagen fibrils and mineral crystallites. Since damage accumulation rate is a highly nonlinear function of stress amplitude [11], it is possible that damage could accumulate at the ultra-structural or micro-structural level even in very short times. However, the expected loss of stiffness as damage accumulates is not evident in the measured stress-strain histories of the SHPB tests, which suggests that local damage does not accumulate to any significant amount prior to failure. Future studies will investigate this issue in more detail.

A limitation of the present study is the single choice of a short cylinder as specimen geometry. The ends of the test samples were lubricated, but it is still possible that the specimen geometry played a role in the outcome of the tests. Although the values of the various parameters might change with another geometry, a single geometry for all tests should insure that the comparisons of behavior are valid.

5. CONCLUSIONS

In summary, we found that samples loaded at high speeds using SHPB demonstrated greatly increased compressive properties compared to statically loaded samples, but failed with extreme abruptness, developing almost complete loss of load carrying capability once ultimate stress was reached. Thus, its ability to absorb further energy beyond that point is very minimal compared to bone which has failed at a rather slow loading rate.

6. REFERENCES

1. Currey, J.D., *Strain rate dependence of the mechanical properties of reindeer antler and the cumulative damage model of bone fracture*. J Biomech, 1989. **22**(5): p. 469-75.
2. Evans, G.P., et al., *The response of equine cortical bone to loading at strain rates experienced in vivo by the galloping horse*. Equine Vet J, 1992. **24**(2): p. 125-8.
3. Wright, T.M. and W.C. Hayes, *Tensile testing of bone over a wide range of strain rates: effects of strain rate, microstructure and density*. Med Biol Eng, 1976. **14**(6): p. 671-80.
4. McElhaney, J.H., *Dynamic response of bone and muscle tissue*. J Appl Physiol, 1966. **21**(4): p. 1231-6.
5. Lewis, J.L. and W. Goldsmith, *The dynamic fracture and prefracture response of compact bone by split Hopkinson bar methods*. J Biomech, 1975. **8**(1): p. 27-40.
6. Burstein, A.H., et al., *Contribution of collagen and mineral to the elastic-plastic properties of bone*. J Bone Joint Surg Am, 1975. **57**(7): p. 956-61.
7. Reilly, D.T. and A.H. Burstein, *The elastic and ultimate properties of compact bone tissue*. J Biomech, 1975. **8**(6): p. 393-405.
8. Burstein, A.H., et al., *The ultimate properties of bone tissue: the effects of yielding*. J Biomech, 1972. **5**(1): p. 35-44.
9. Fondrk, M., et al., *Some viscoplastic characteristics of bovine and human cortical bone*. J Biomech, 1988. **21**(8): p. 623-30.
10. Fondrk, M.T., E.H. Bahniuk, and D.T. Davy, *Inelastic strain accumulation in cortical bone during rapid transient tensile loading*. J Biomech Eng, 1999. **121**(6): p. 616-21.
11. Caler, W.E. and D.R. Carter, *Bone creep-fatigue damage accumulation*. J Biomech, 1989. **22**(6-7): p. 625-35.

7. ACKNOWLEDGEMENTS

This work was supported in part by NIH Grants AR43785 and NIH AR07505. Equine bone was generously provided by the Ohio State University College of Veterinary Medicine.